Joint Beam Training and Positioning for Intelligent Reflecting Surfaces Assisted Millimeter Wave Communications

Dr. Wei Wang

The School of Electrical Engineering & Telecommunications
The University of New South Wales, Sydney, Australia

17 Jan. 2021

Outline

- ❑ Background and Motivation
- ❑ System Model
- ❑ Beam Training and Positioning
- ❑ Numerical Results
- ❑ Conclusion

Evolution from 1G to 5G

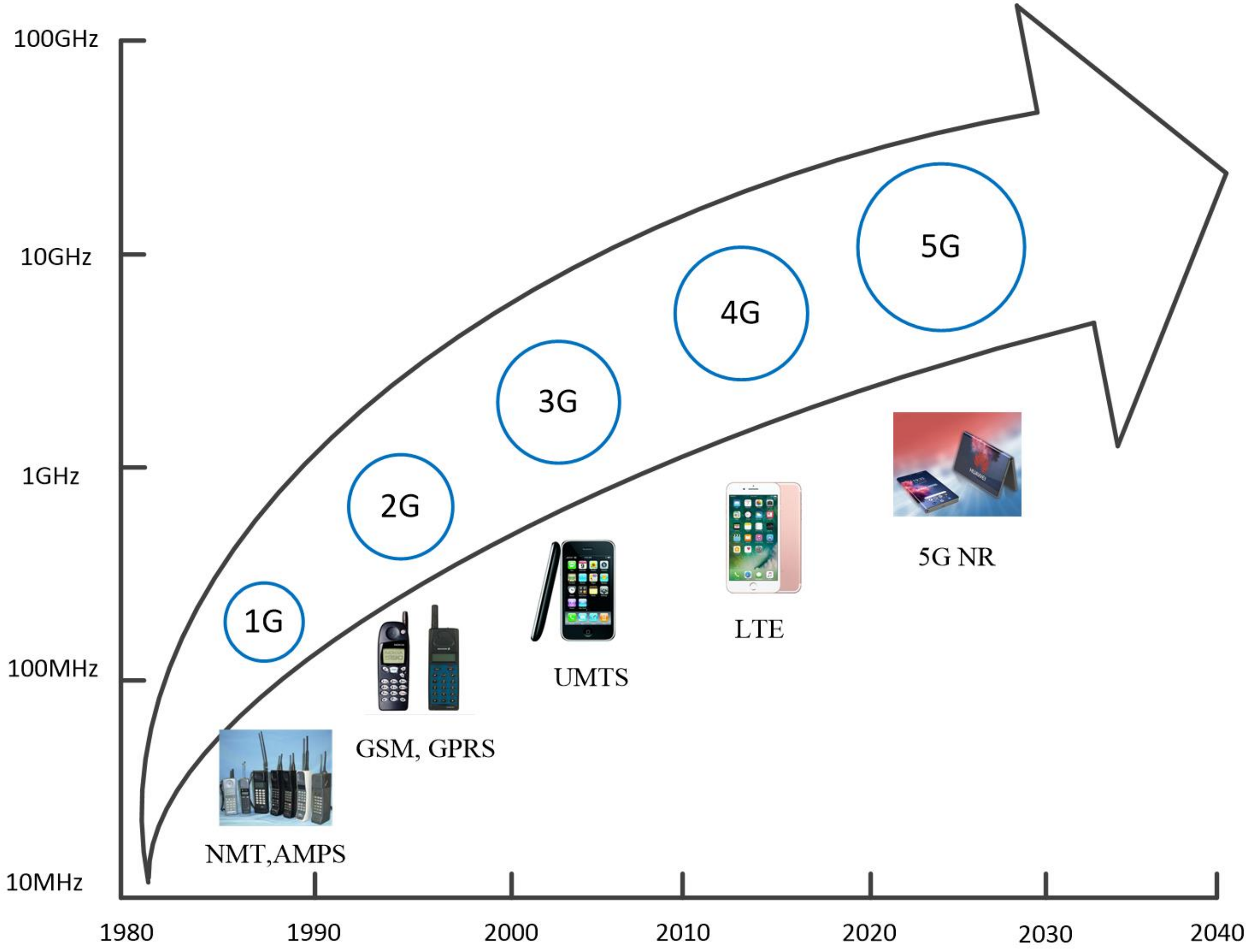

Evolution from 1G to 5G

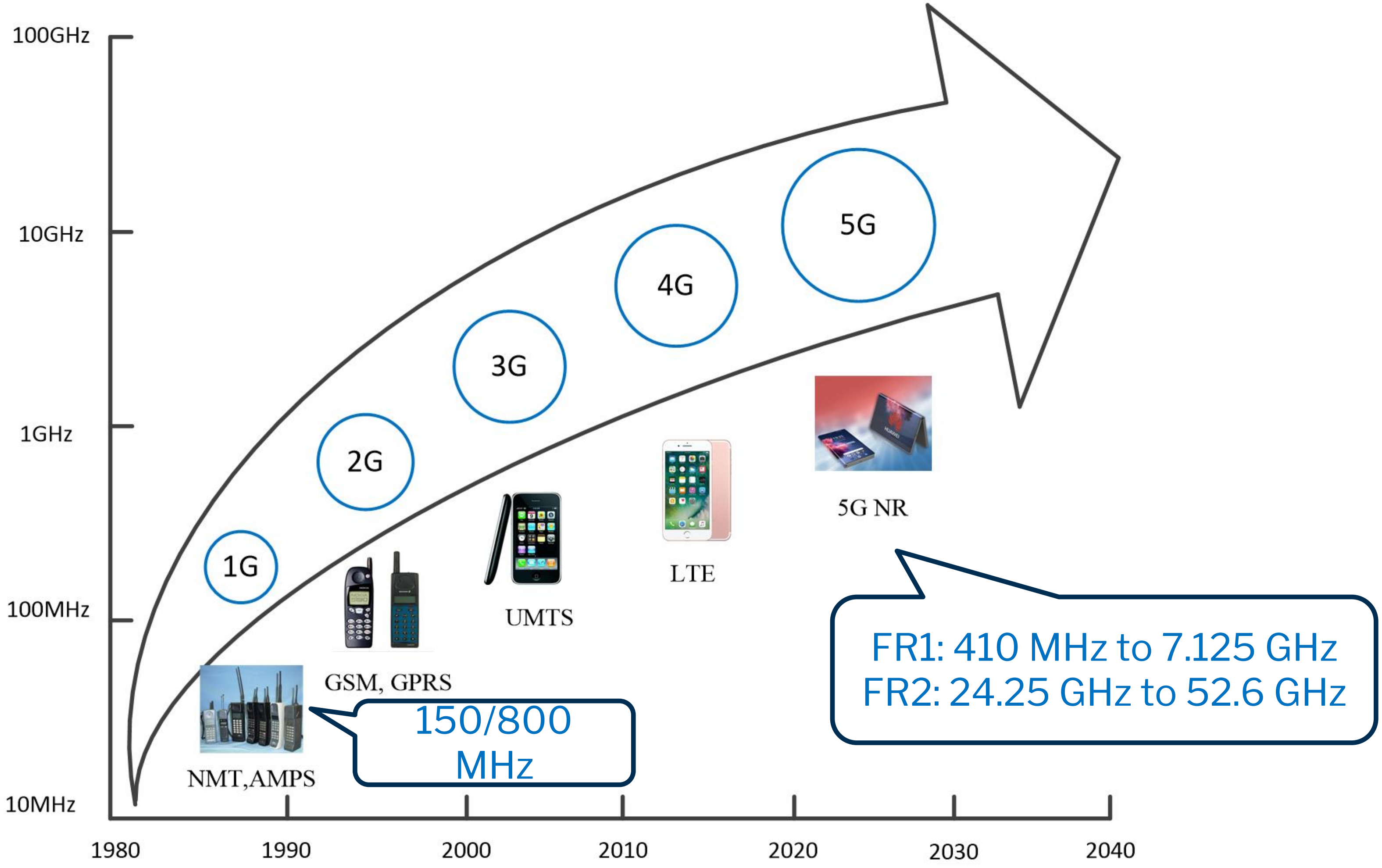

Evolution from 1G to 5G

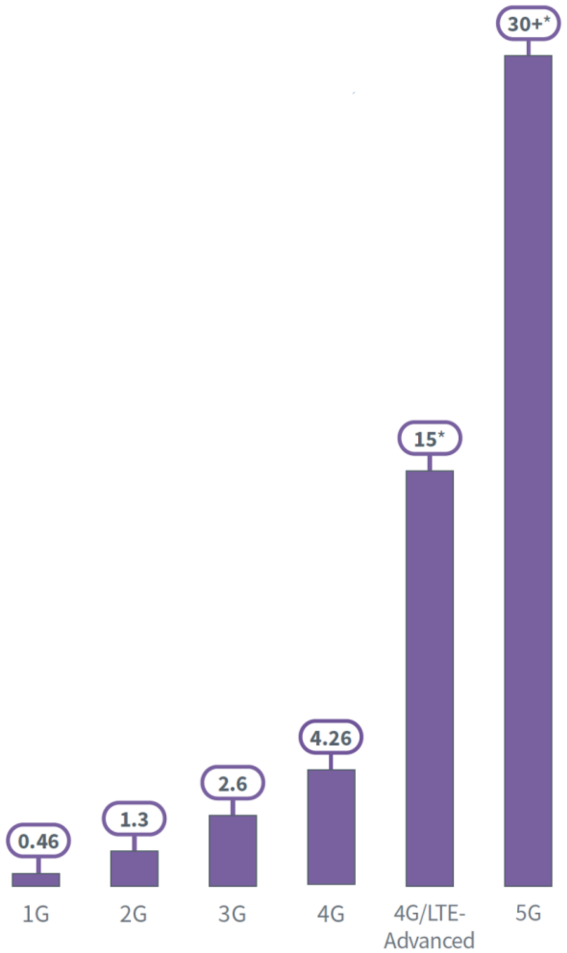

Fig. 1 Spectral efficiency by wireless generation (bps/Hz), * indicates standards peak targets [1]

[1] CTIA report, "Smarter and More Efficient: How America's Wireless Industry Maximizes its Spectrum"

Evolution from 1G to 5G

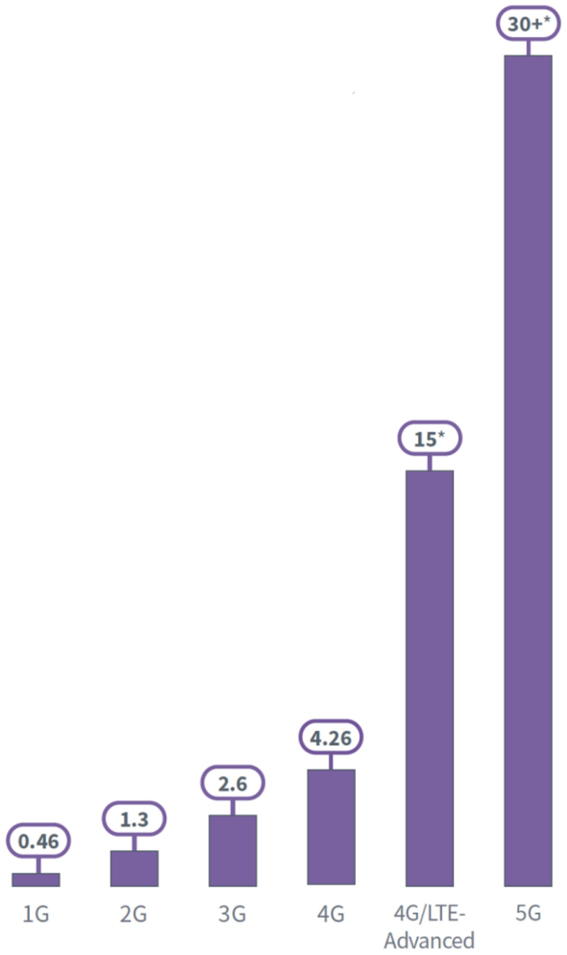

Fig. 1 Spectral efficiency by wireless generation (bps/Hz), * indicates standards peak targets [1]

❖ Shannon–Hartley theorem

$$C = \underbrace{B}_{\text{bandwidth}} \underbrace{\log_2 \det(\mathbf{I}_{N_r} + \frac{\mathbf{H}\mathbf{K}_x\mathbf{H}^H}{\sigma_n^2})}_{\text{spectral efficiency}}$$

[1] CTIA report, “Smarter and More Efficient: How America's Wireless Industry Maximizes its Spectrum”

Evolution from 1G to 5G

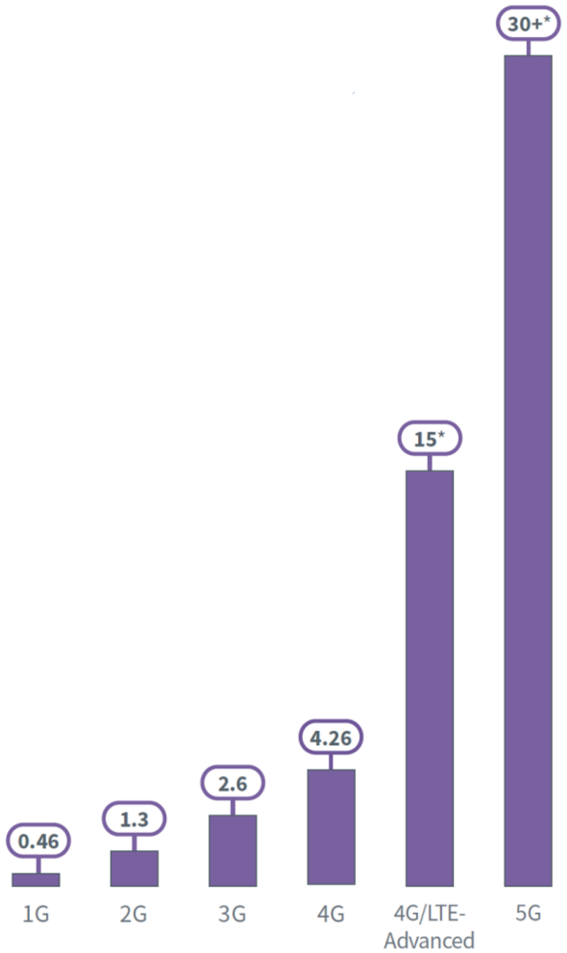

Fig. 1 Spectral efficiency by wireless generation (bps/Hz), * indicates standards peak targets [1]

- Shannon–Hartley theorem

$$C = \underbrace{B}_{\text{bandwidth}} \underbrace{\log_2 \det(\mathbf{I}_{N_r} + \frac{\mathbf{H}\mathbf{K}_x\mathbf{H}^H}{\sigma_n^2})}_{\text{spectral efficiency}}$$

- Bandwidth
  - Proportional to operating frequency

[1] CTIA report, “Smarter and More Efficient: How America's Wireless Industry Maximizes its Spectrum”

Evolution from 1G to 5G

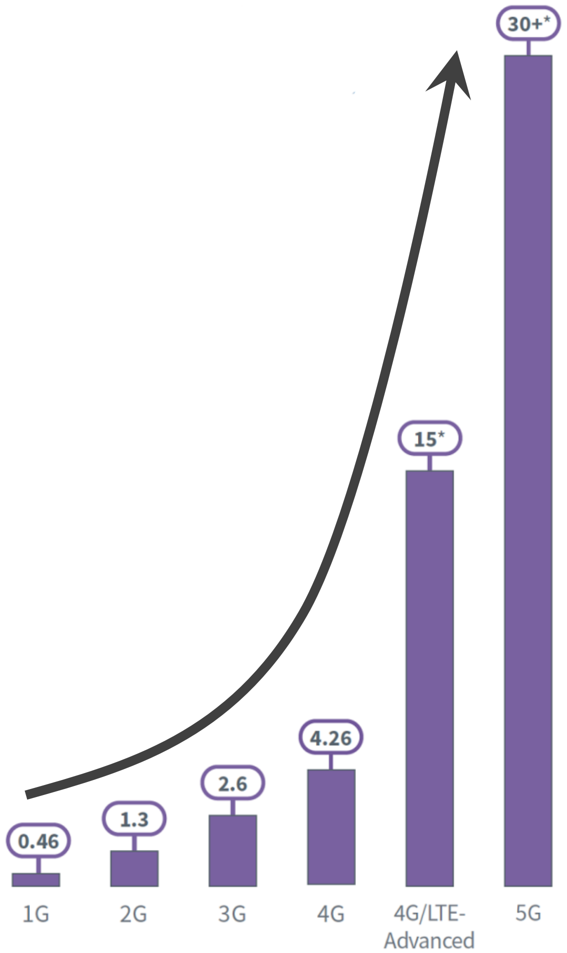

Fig. 1 Spectral efficiency by wireless generation (bps/Hz), * indicates standards peak targets [1]

- ❖ Shannon–Hartley theorem

$$C = \underbrace{B}_{\text{bandwidth}} \underbrace{\log_2 \det\left(\mathbf{I}_{N_r} + \frac{\mathbf{H}\mathbf{K}_x\mathbf{H}^H}{\sigma_n^2}\right)}_{\text{spectral efficiency}}$$

- ❖ Bandwidth
  - Proportional to operating frequency
- ❖ Spectral efficiency
  - MIMO technology applied to 4G, 5G and future generations.

[1] CTIA report, “Smarter and More Efficient: How America's Wireless Industry Maximizes its Spectrum”

Millimeter wave (mmWave) communications

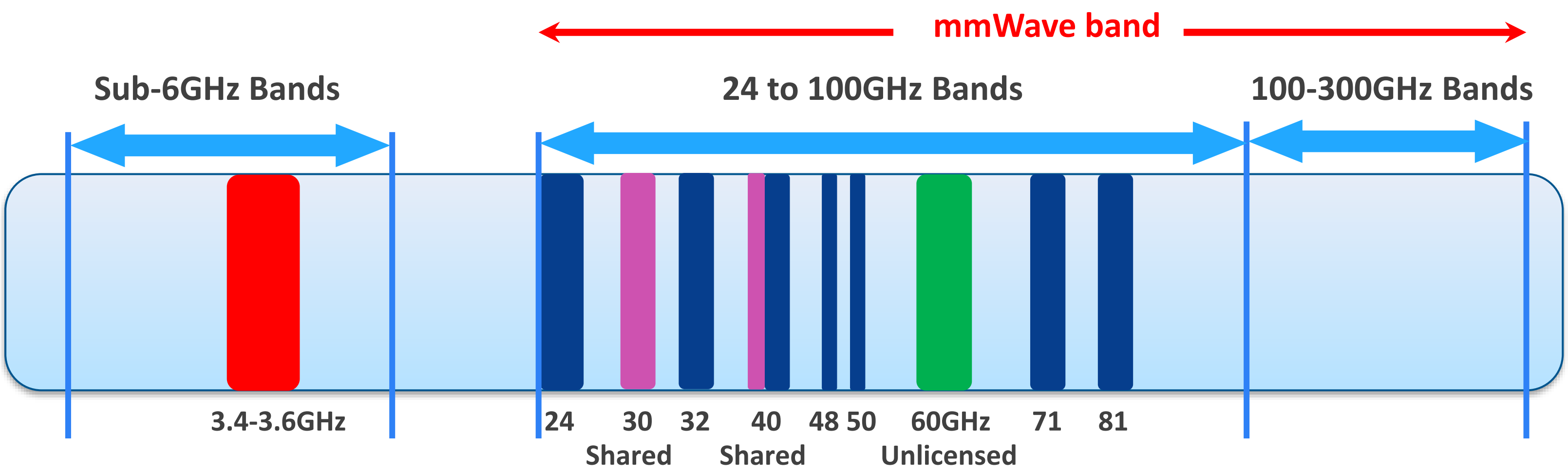

Millimeter wave (mmWave) communications

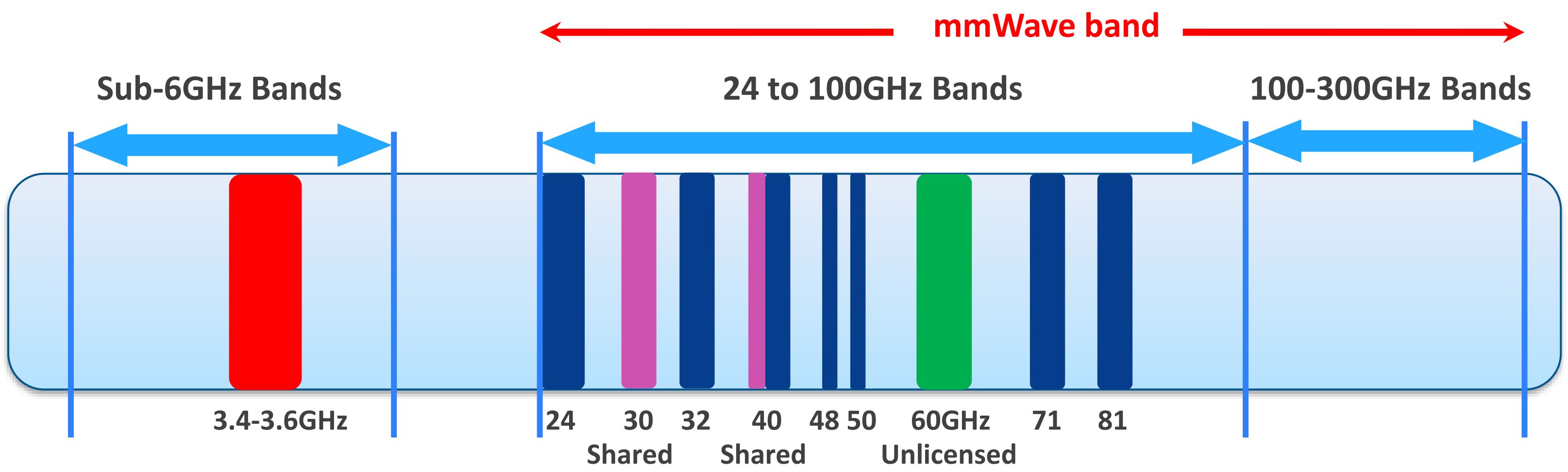

- Opportunities
  - Abundant spectrum resources
  - Compact massive MIMO antennas

Millimeter wave (mmWave) communications

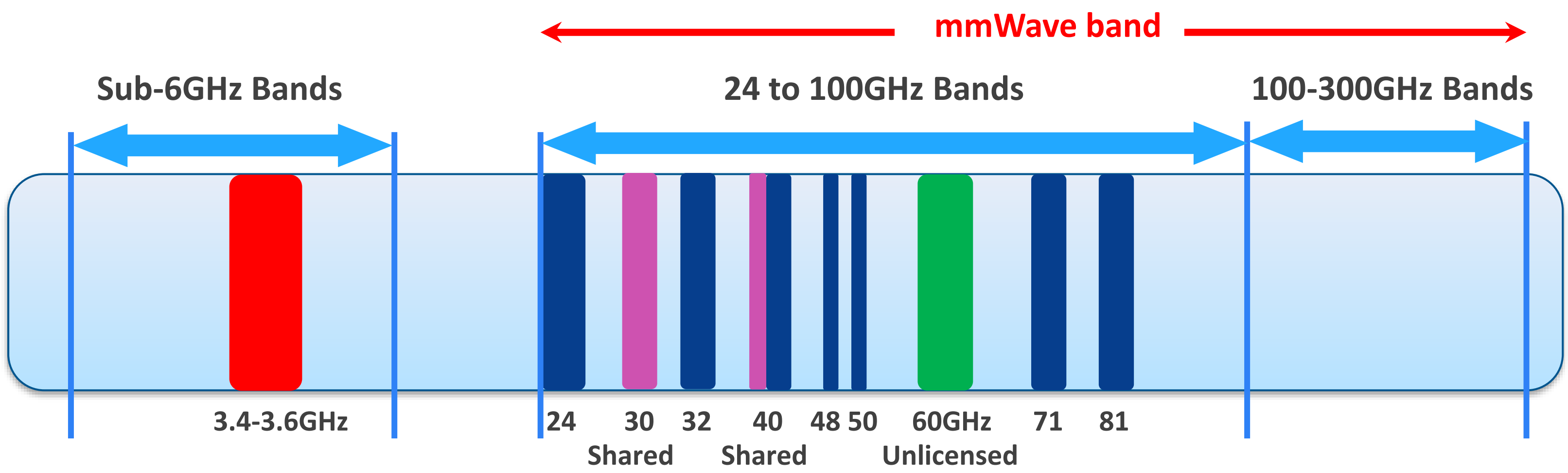

- Opportunities
  - Abundant spectrum resources
  - Compact massive MIMO antennas

- Challenges
  - High propagation loss
    - LoS dominant
  - Vulnerable to blockage

MIMO channel in richly scattered environment

— The ideal case

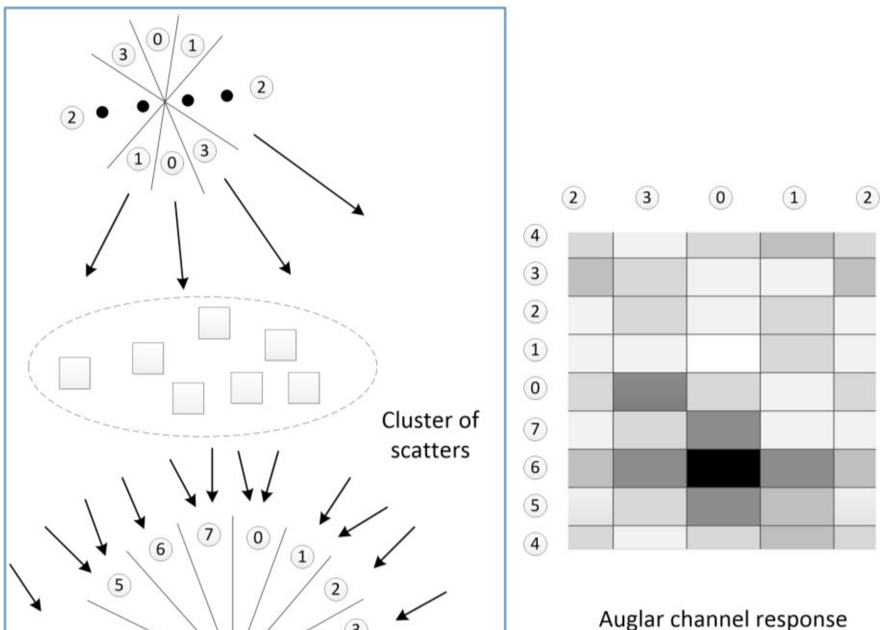

Fig. 2 MIMO channel in angular domain [2] in richly scattered environment

[2] Tse, David, and Pramod Viswanath. Fundamentals of wireless communication. Cambridge university press, 2005.

MIMO channel in richly scattered environment
— The ideal case

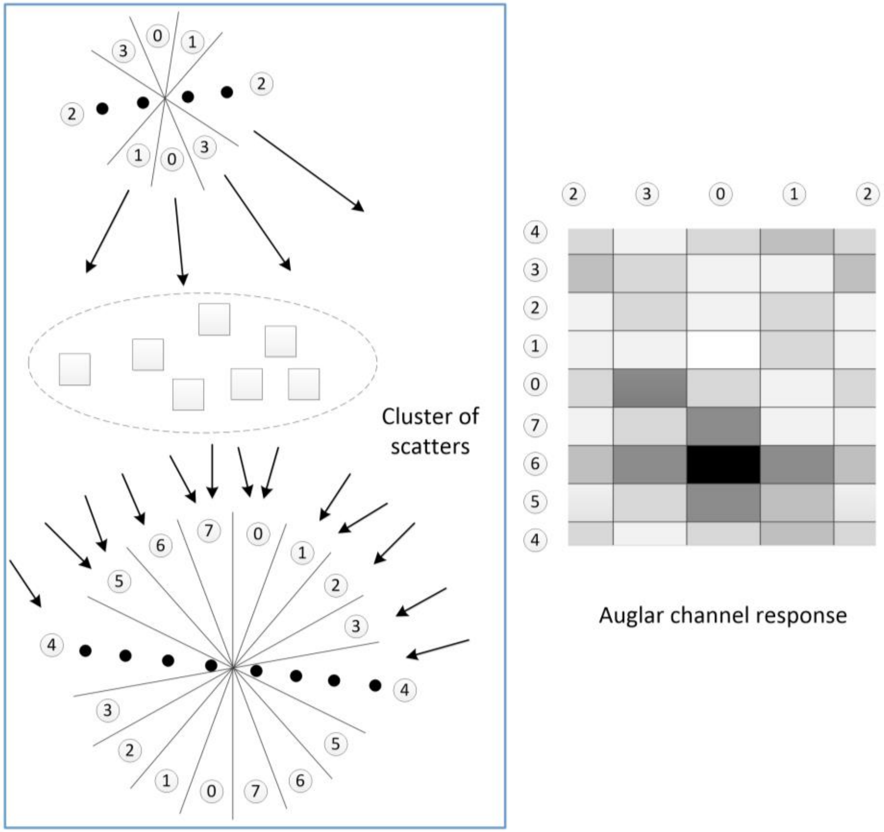

Fig. 2 MIMO channel in angular domain [2] in richly scattered environment

- Full angular spread
- Well-conditioned channel
- Rayleigh fading/ Rician fading

[2] Tse, David, and Pramod Viswanath. Fundamentals of wireless communication. Cambridge university press, 2005.

MIMO channel in poorly scattered environment
— MmWave communications

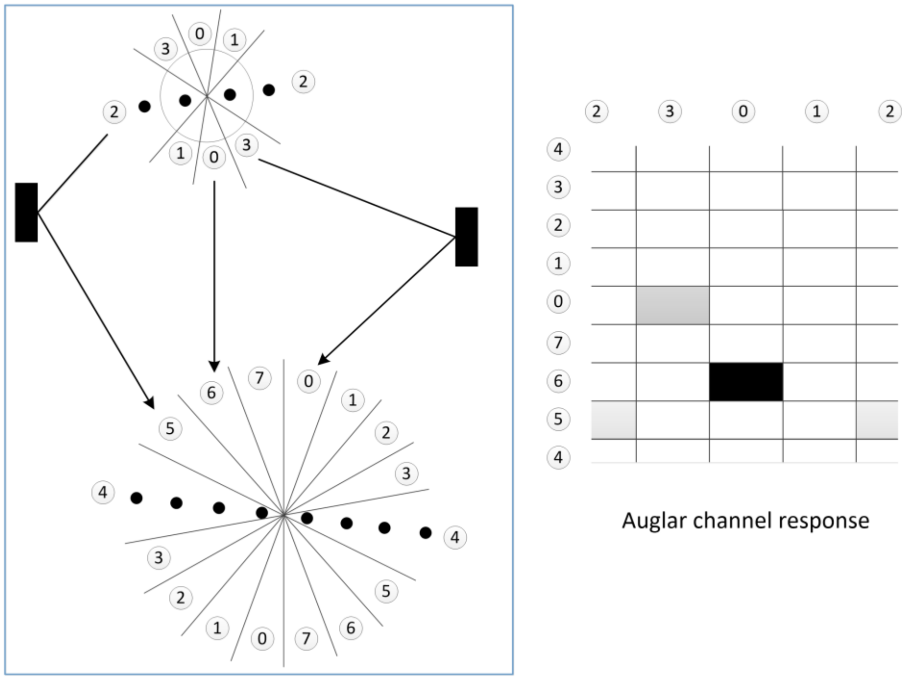

Fig. 3 MmWave MIMO channel in angular domain

MIMO channel in poorly scattered environment
— MmWave communications

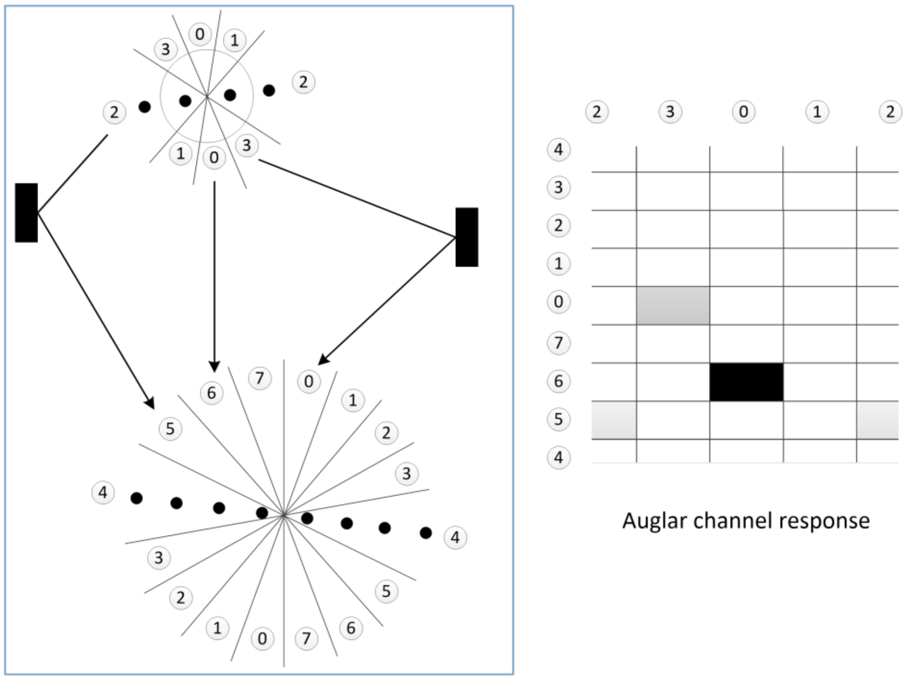

Fig. 3 MmWave MIMO channel in angular domain

- Small angular spread
- ILL-conditioned channel
  - Limited degree-of-freedom gain
- Vulnerable to blockage

MIMO channel in poorly scattered environment
— MmWave communications

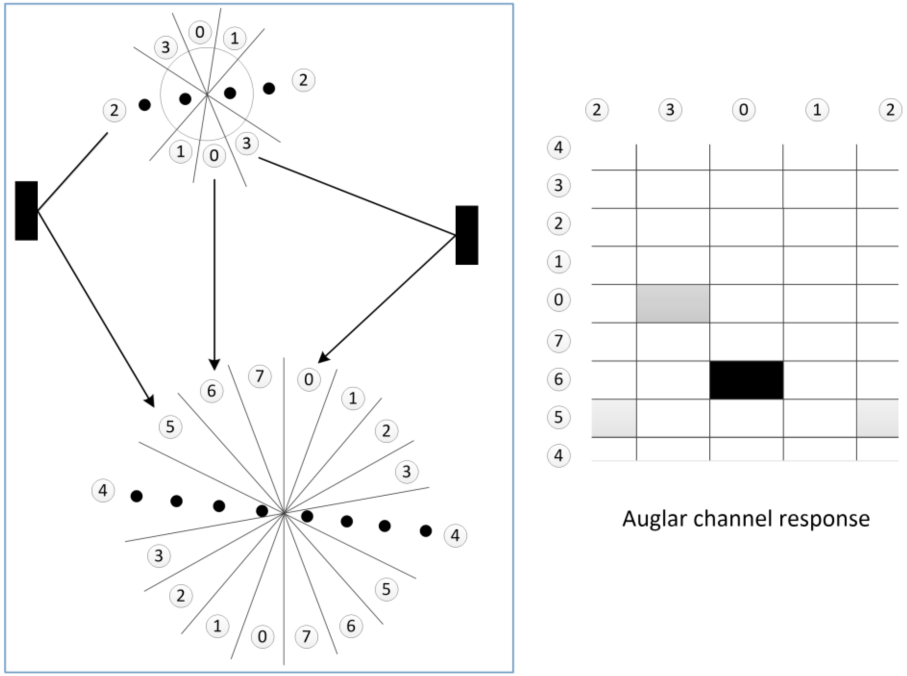

Fig. 3 MmWave MIMO channel in angular domain

- Small angular spread
- ILL-conditioned channel
  - Limited degree-of-freedom gain
- Vulnerable to blockage

Can mmWave channel be improved artificially?

Intelligent Reflecting Surface (IRS)

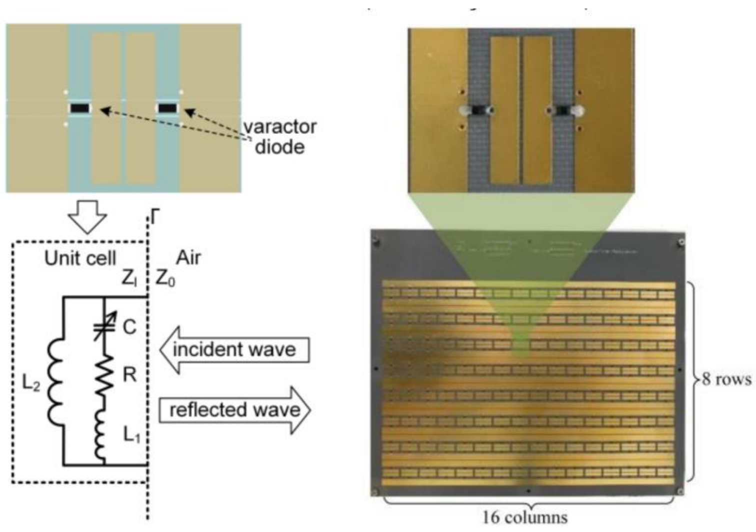

Fig. 4 Fabricated programmable metasurface and the simplified equivalent circuit model [3]

Metamaterials – A breakthrough in material science

- Metasurfaces, two-dimensional metasurfaces;
- Massive low-cost reflecting elements mounted on a planar surface;
- Passive, no RF energy consumption, negligible additive noise [4].

[3] W. Tang, et al. "Wireless communications with programmable metasurface: Transceiver design and experimental results." China Communications 16.5 (2019): 46-61.
[4] M. Di Renzo et al., "Reconfigurable intelligent surfaces vs. relaying: Differences, similarities, and performance comparison," in IEEE Open Journal of the Communications Society, vol. 1, pp. 798-807, 2020.

Outline

- ❑ Background and Motivation
- ❑ System Model
- ❑ Beam Training and Positioning
- ❑ Numerical Results
- ❑ Conclusion

MmWave channel

Channel response of mmWave communications

$$\mathbf{H} = \underbrace{\zeta_{LoS}\delta_1 \mathbf{a}_M(\theta_{BM,1})\mathbf{a}_B^H(\phi_{BM,1})}_{LoS\ component} + \underbrace{\sum_{l=2}^{L} \delta_l \mathbf{a}_M(\theta_{BM,l})\mathbf{a}_B^H(\phi_{BM,l})}_{NLoS\ component}$$

1. ζ_{LoS} is the indicator of blockage
2. δ_l is the path coefficient
3. $\theta_{BM,l}, \phi_{BM,l}$ are cosine AoA and cosine AoD
4. $\mathbf{a}_M(\cdot), \mathbf{a}_B(\cdot)$steering vectors in mobile terminal's side and base station's side.
5. The number of paths L is a small number, and that power of the LoS component is about 13 dB higher than the sum of power of NLoS components [5] .

[5] Z. Muhi-Eldeen, L. Ivrissimtzis, and M. Al-Nuaimi, "Modelling and measurements of millimetre wavelength propagation in urban environments," *IET Microw., Antennas Propag.*, vol. 4, no. 9, pp. 1300–1309, 2010.

MmWave channel assisted by IRSs

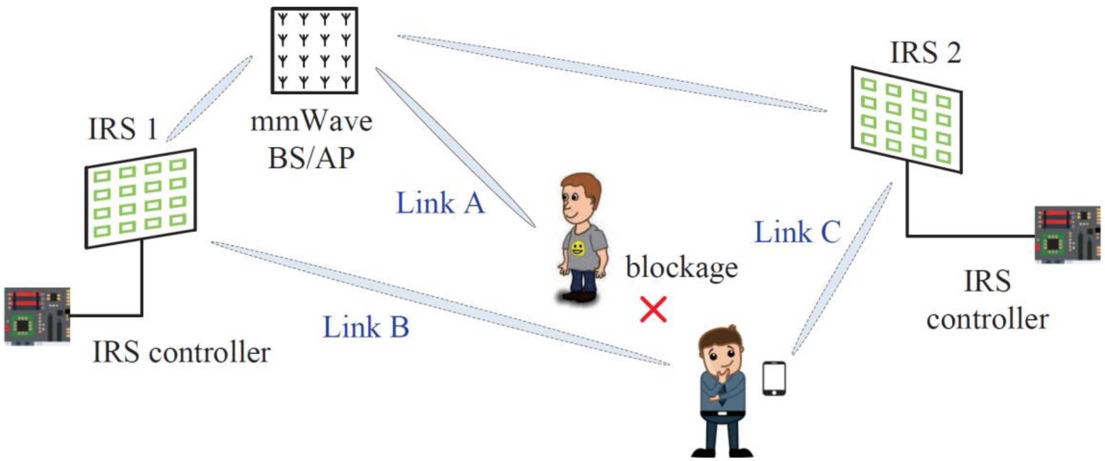

Channel response of mmWave communications assisted by IRSs

$$\mathbf{H} = \underbrace{\zeta_{LoS}\delta_1 \mathbf{a}_M(\theta_{BM,1})\mathbf{a}_B^H(\phi_{BM,1})}_{LoS\ component} + \underbrace{\sum_{l=2}^{L} \delta_l \mathbf{a}_M(\theta_{BM,l})\mathbf{a}_B^H(\phi_{BM,l})}_{NLoS\ component}$$

$$+ \underbrace{\sum_{i=1}^{N_{IRS}} \gamma_i \zeta_{VLoS,i} \delta_{BR_iM}(\bar{\mathbf{g}}_i)\mathbf{a}_M(\theta_{R_iM})\mathbf{a}_B^H(\phi_{BR_i})}_{VLoS\ component}$$

MmWave channel assisted by IRSs

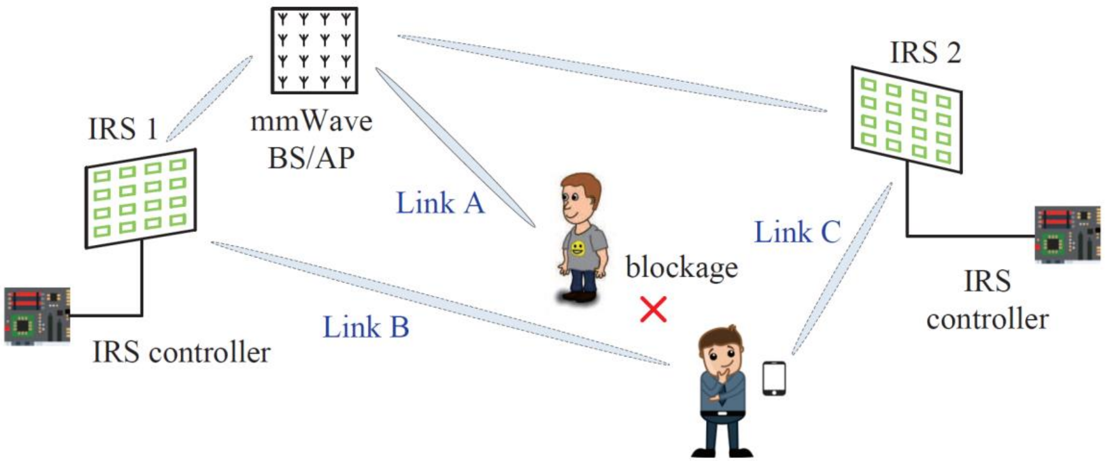

Channel response of mmWave communications assisted by IRSs

$$\mathbf{H} = \underbrace{\zeta_{LoS}\delta_1 \mathbf{a}_M(\theta_{BM,1})\mathbf{a}_B^H(\phi_{BM,1})}_{LoS\ component} + \underbrace{\sum_{l=2}^{L} \delta_l \mathbf{a}_M(\theta_{BM,l})\mathbf{a}_B^H(\phi_{BM,l})}_{NLoS\ component}$$

$$+ \underbrace{\sum_{i=1}^{N_{IRS}} \gamma_i \zeta_{VLoS,i}\delta_{BR_iM}(\bar{\mathbf{g}}_i)\mathbf{a}_M(\theta_{R_iM})\mathbf{a}_B^H(\phi_{BR_i})}_{VLoS\ component}$$

IRSs should be dispersedly placed to increase angular spread

Optimal reflection pattern

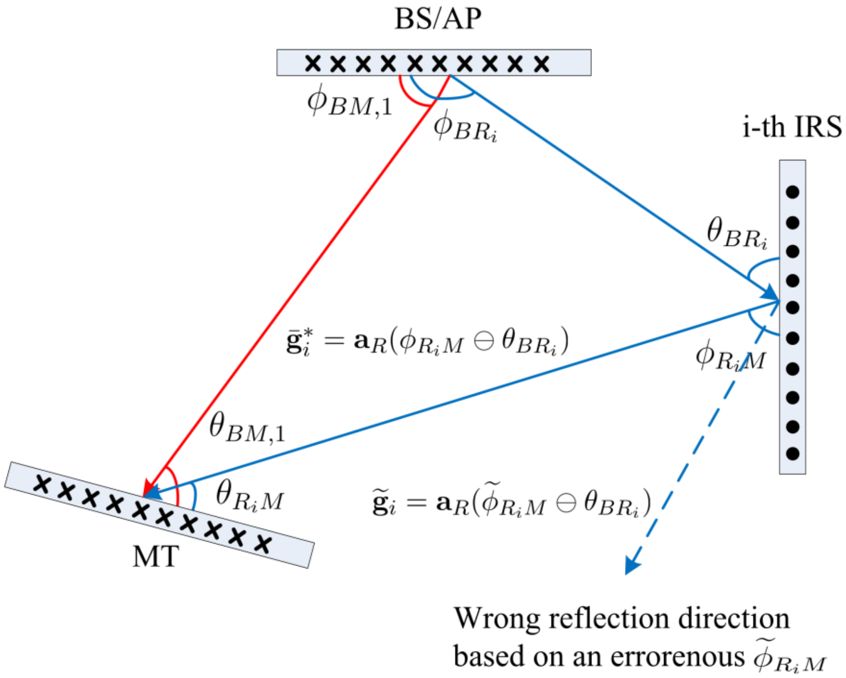

Fig. 5 Illustration of LoS/VLoS related AoAs/AoDs

Optimal reflection pattern

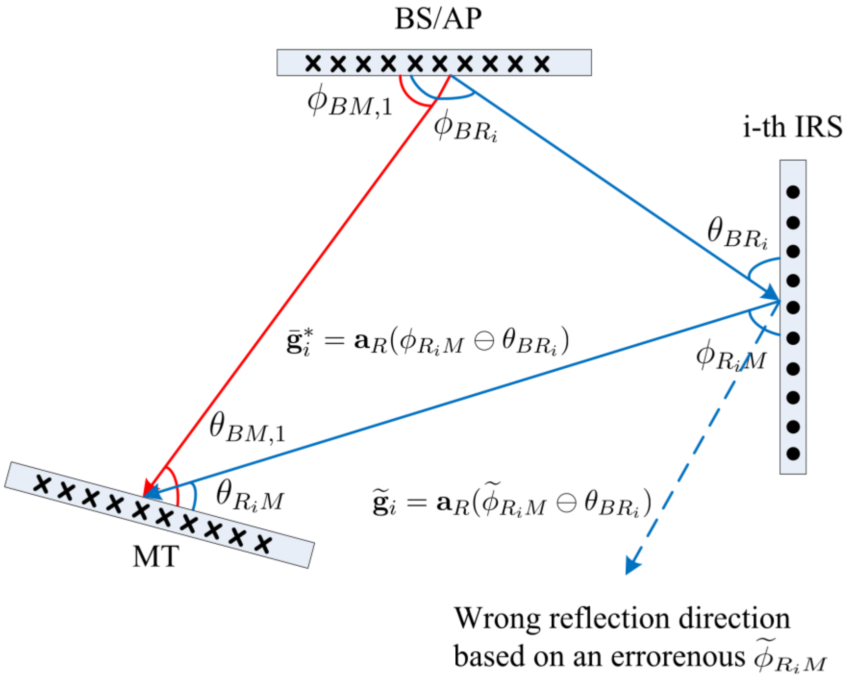

Fig. 5 Illustration of LoS/VLoS related AoAs/AoDs

- $\delta_{BR_iM}(\bar{\mathbf{g}}_i)$ is the equivalent path gain of the i-th virtual LoS (VLoS), i.e.,

$$\begin{aligned}\delta_{BR_iM}(\bar{\mathbf{g}}_i) &\triangleq \bar{\delta}_{BR_iM}\mathbf{a}_{R_i}^H(\phi_{R_iM})\{\bar{\mathbf{g}}_i\}\mathbf{a}_{R_i}(\theta_{BR_i}) \\ &= \bar{\delta}_{BR_iM}\mathbf{a}_{R_i}^H(\phi_{R_iM} \ominus \theta_{BR_i})\bar{\mathbf{g}}_i\end{aligned}$$

Optimal reflection pattern

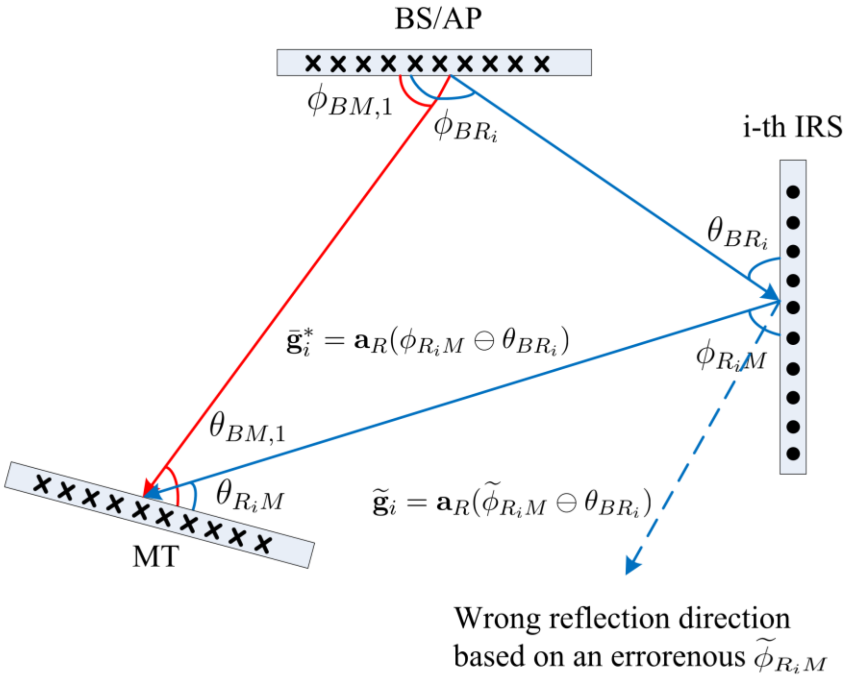

Fig. 5 Illustration of LoS/VLoS related AoAs/AoDs

- $\delta_{BR_iM}(\bar{\mathbf{g}}_i)$ is the equivalent path gain of the i-th virtual LoS (VLoS), i.e.,

$$\begin{aligned}\delta_{BR_iM}(\bar{\mathbf{g}}_i) &\triangleq \bar{\delta}_{BR_iM}\mathbf{a}_{R_i}^H(\phi_{R_iM})\{\bar{\mathbf{g}}_i\}\mathbf{a}_{R_i}(\theta_{BR_i}) \\ &= \bar{\delta}_{BR_iM}\mathbf{a}_{R_i}^H(\phi_{R_iM} \ominus \theta_{BR_i})\bar{\mathbf{g}}_i\end{aligned}$$

- The optimal reflection pattern is

$$\bar{\mathbf{g}}_i^* = \mathbf{a}_R(\phi_{R_iM} \ominus \theta_{BR_i})$$

Optimal reflection pattern

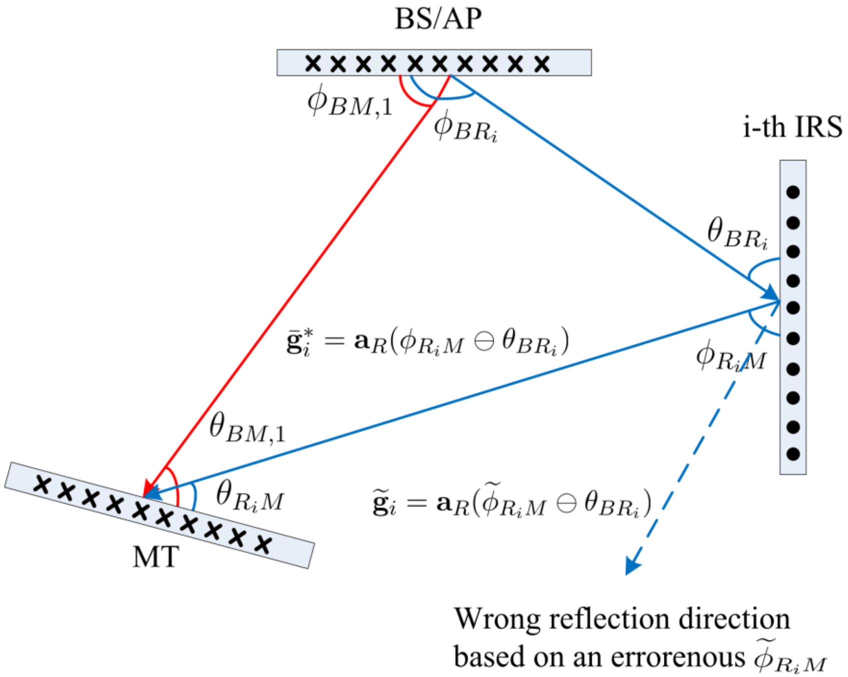

Fig. 5 Illustration of LoS/VLoS related AoAs/AoDs

- $\delta_{BR_iM}(\bar{\mathbf{g}}_i)$ is the equivalent path gain of the i-th virtual LoS (VLoS), i.e.,

$$\delta_{BR_iM}(\bar{\mathbf{g}}_i) \triangleq \bar{\delta}_{BR_iM}\mathbf{a}_{R_i}^H(\phi_{R_iM})\{\bar{\mathbf{g}}_i\}\mathbf{a}_{R_i}(\theta_{BR_i}) = \bar{\delta}_{BR_iM}\mathbf{a}_{R_i}^H(\phi_{R_iM} \ominus \theta_{BR_i})\bar{\mathbf{g}}_i$$

- The optimal reflection pattern is

$$\bar{\mathbf{g}}_i^* = \mathbf{a}_R(\phi_{R_iM} \ominus \theta_{BR_i})$$

- Knowledge of $\phi_{BM,1}, \theta_{BM,1}$ and $\phi_{R_i,M}, \theta_{R_iM}$ are essential for beamforming designs.

Outline

- ❑ Background and Motivation
- ❑ System Model
- ❑ Beam Training and Positioning
- ❑ Numerical Results
- ❑ Conclusion

Breakdown of beam training

Unlike scatterers/reflectors in physical world, IRSs can be controlled to meet our needs

Breakdown of beam training

Unlike scatterers/reflectors in physical world, IRSs can be controlled to meet our needs

- More activated IRSs are favourable in data transmission stage;
  - Better channel condition
  - Less sparse in angular domain

Breakdown of beam training

Unlike scatterers/reflectors in physical world, IRSs can be controlled to meet our needs

- ❖ More activated IRSs are favourable in data transmission stage;
  - Better channel condition
  - Less sparse in angular domain
- ❖ Less activated IRSs are favourable in beam training stage;
  - Poor channel condition
  - Sparse in angular domain
    - Compressed sensing, sparser → more solvable

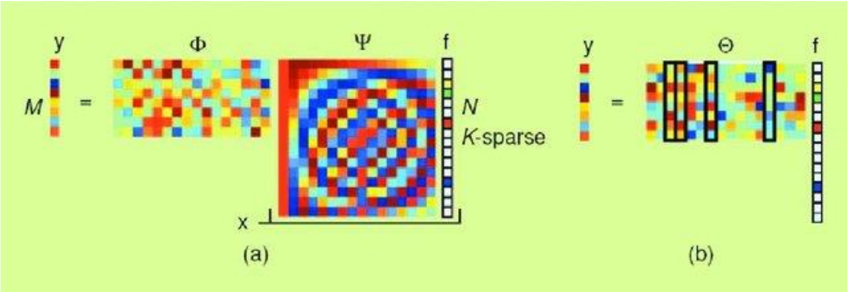

Breakdown of beam training

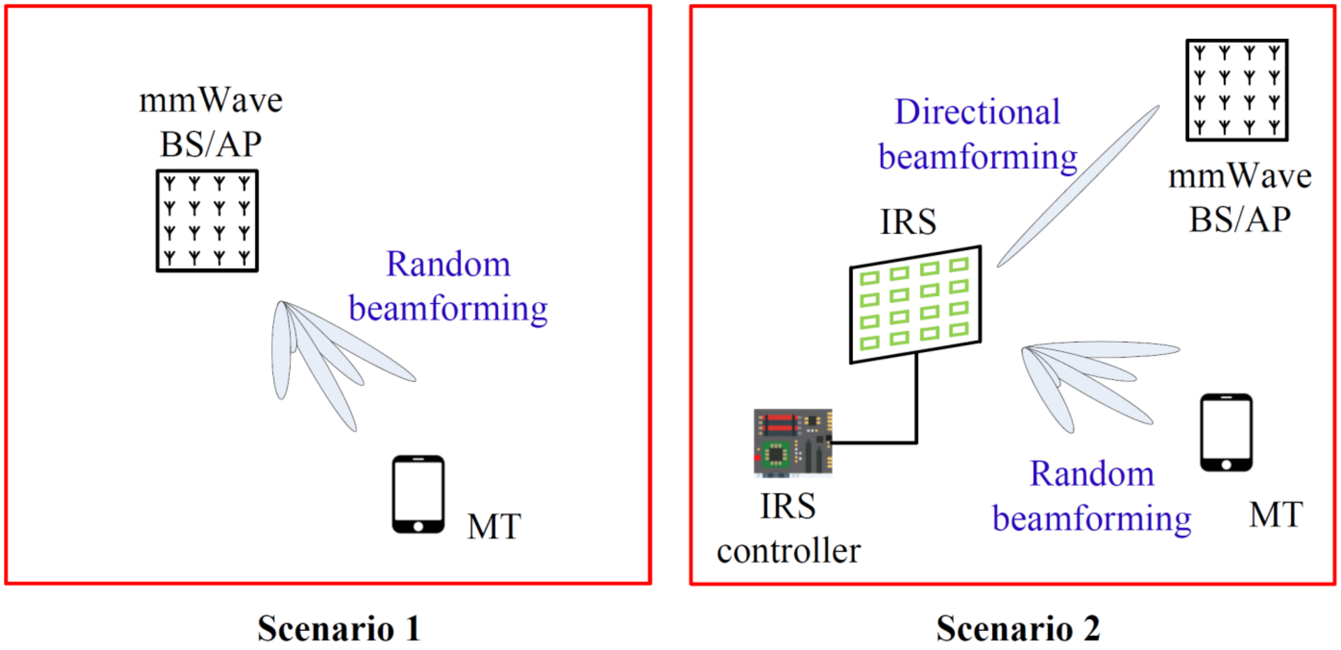

❖ In Scenario 2, BS/AP works as a feed antenna to provide incident wave

Parameter estimation of an LoS/VLoS path

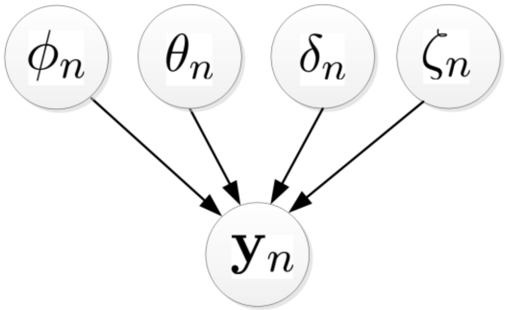

- The unified signal model in Scenario 1&2

$$\mathbf{y}_n = \zeta_n \delta_n \mathbf{D}\mathbf{b}(\theta_n, \phi_n) + \mathbf{w}$$

ζ_n : indicator of blockage

δ_n : path coefficient

θ_n : cosine AoA

ϕ_n: cosine AoD

$\mathbf{y}_n$: channel measurements

Parameter estimation of an LoS/VLoS path

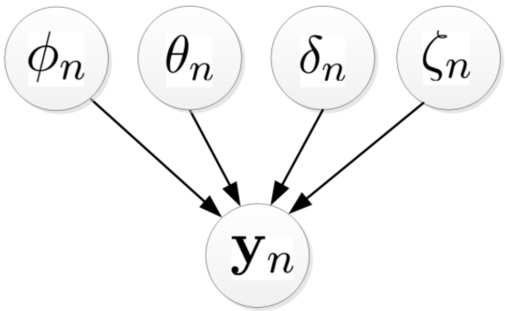

- The unified signal model in Scenario 1&2

$$\mathbf{y}_n = \zeta_n \delta_n \mathbf{D}\mathbf{b}(\theta_n, \phi_n) + \mathbf{w}$$

- Estimation of $\delta_n, \theta_n, \phi_n$ under the assumption $\zeta_n = 1$

$$(\hat{\delta}_n, \hat{\theta}_n, \hat{\phi}_n) = \mathrm{argmax}_{\delta_n, \theta_n, \phi_n} \mathcal{L}(\delta_n, \theta_n, \phi_n)$$

where $\mathcal{L}(\delta_n, \theta_n, \phi_n) = \log P(\mathbf{y} | \zeta_n = 1, \delta_n, \theta_n, \phi_n)$

ζ_n : indicator of blockage

δ_n : path coefficient

θ_n : cosine AoA

ϕ_n: cosine AoD

$\mathbf{y}_n$: channel measurements

Parameter estimation of an LoS/VLoS path

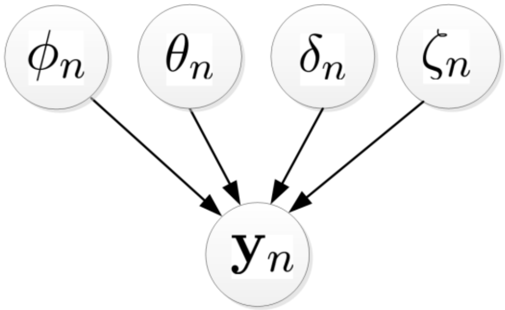

ζ_n : indicator of blockage

δ_n : path coefficient

θ_n : cosine AoA

ϕ_n: cosine AoD

$\mathbf{y}_n$: channel measurements

- The unified signal model in Scenario 1&2

$$\mathbf{y}_n = \zeta_n \delta_n \mathbf{D}\mathbf{b}(\theta_n, \phi_n) + \mathbf{w}$$

- Estimation of $\delta_n, \theta_n, \phi_n$ under the assumption $\zeta_n = 1$

$$(\hat{\delta}_n, \hat{\theta}_n, \hat{\phi}_n) = \text{argmax}_{\delta_n, \theta_n, \phi_n} \mathcal{L}(\delta_n, \theta_n, \phi_n)$$

where $\mathcal{L}(\delta_n, \theta_n, \phi_n) = \log P(\mathbf{y} | \zeta_n = 1, \delta_n, \theta_n, \phi_n)$

- Estimation of blockage indicator ζ_n
  - Residual signal power ratio

$$\varpi_n = \frac{\|\mathbf{y}_n - \hat{\delta}_n \mathbf{D}\mathbf{b}(\hat{\theta}_n, \hat{\phi}_n)\|_2^2}{\|\mathbf{y}_n\|_2^2}$$

  - How well the estimated $(\hat{\delta}_n, \hat{\theta}_n, \hat{\phi}_n)$ can reconstruct channel measurements $\mathbf{y}_n$

Interplay between beam training and positioning

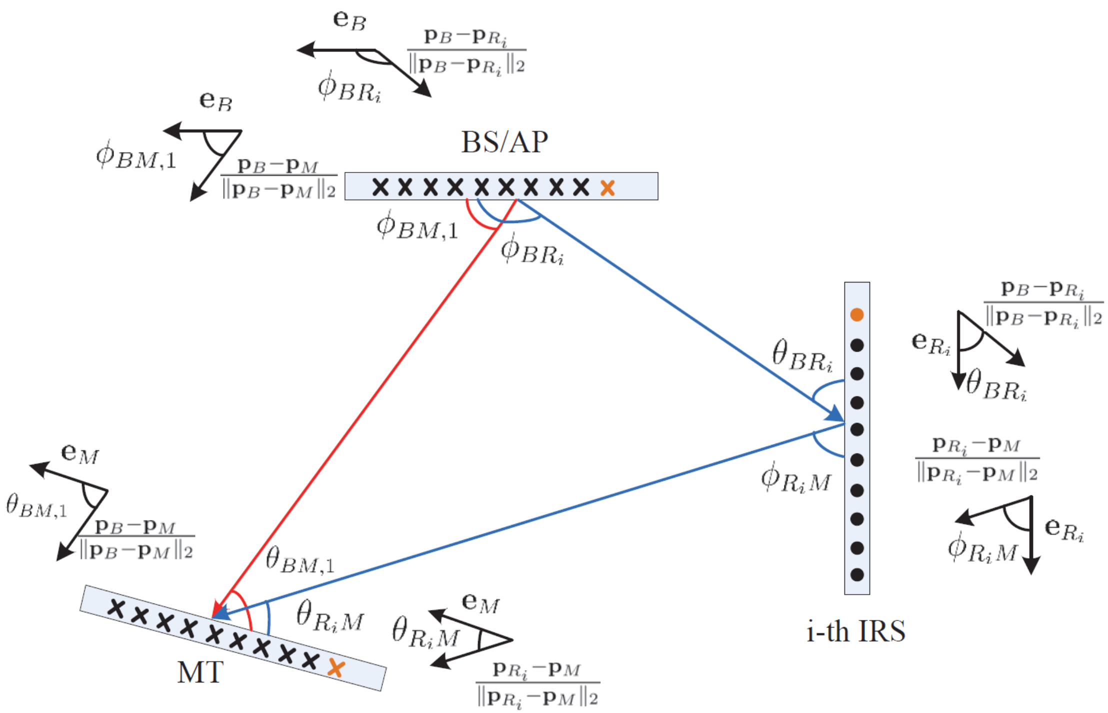

$\mathbf{e}_B$	Direction vector of the ULA of BS/AP
$\mathbf{e}_{R_i}$	Direction vector of the ULA of the i-th IRS
$\mathbf{e}_M$	Direction vector of the ULA of MT
$\mathbf{p}_B$	Position of BS/AP
$\mathbf{p}_{R_i}$	Position of the i-th IRS
$\mathbf{p}_M$	Position of MT

Interplay between beam training and positioning

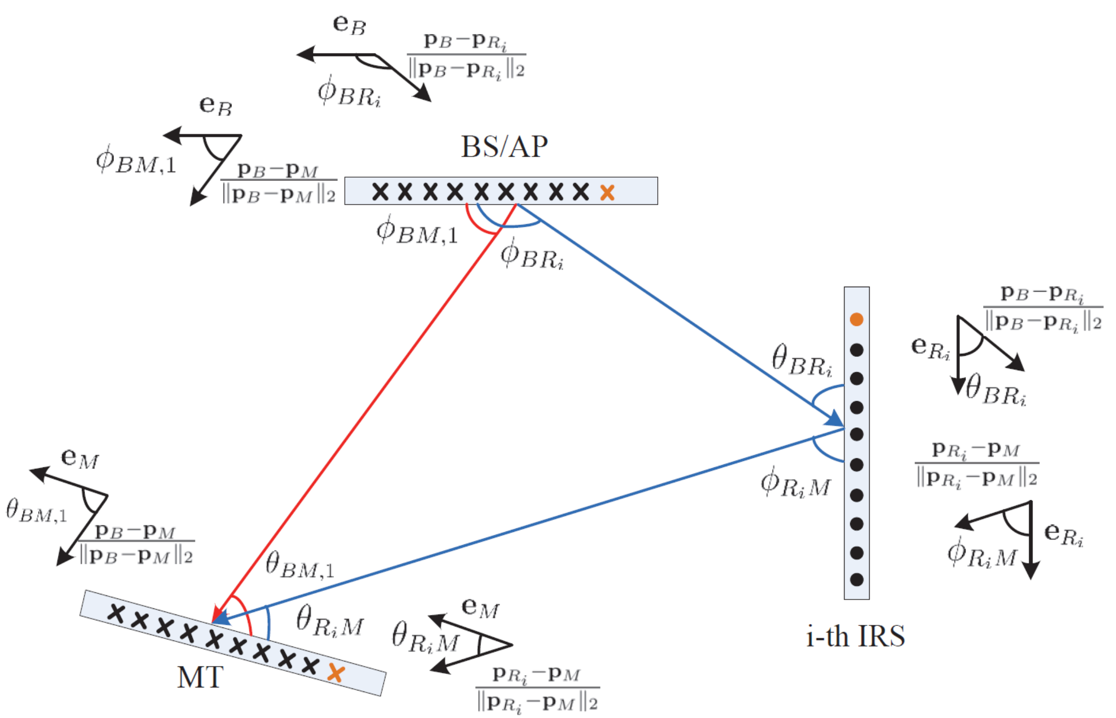

$\mathbf{e}_B$	Direction vector of the ULA of BS/AP
$\mathbf{e}_{R_i}$	Direction vector of the ULA of the i-th IRS
$\mathbf{e}_M$	Direction vector of the ULA of MT
$\mathbf{p}_B$	Position of BS/AP
$\mathbf{p}_{R_i}$	Position of the i-th IRS
$\mathbf{p}_M$	Position of MT

LoS/VLoS path parameters are MT location dependent

$$\phi_{BM,1} = \frac{(\mathbf{p}_B - \mathbf{p}_M)^T}{\|\mathbf{p}_B - \mathbf{p}_M\|_2}\mathbf{e}_B, \quad \phi_{R_iM} = \frac{(\mathbf{p}_{R_i} - \mathbf{p}_M)^T}{\|\mathbf{p}_{R_i} - \mathbf{p}_M\|_2}\mathbf{e}_{R_i}$$

$$\theta_{BM,1} = \frac{(\mathbf{p}_B - \mathbf{p}_M)^T}{\|\mathbf{p}_B - \mathbf{p}_M\|_2}\mathbf{e}_M, \quad \theta_{R_iM} = \frac{(\mathbf{p}_{R_i} - \mathbf{p}_M)^T}{\|\mathbf{p}_{R_i} - \mathbf{p}_M\|_2}\mathbf{e}_M$$

Interplay between beam training and positioning

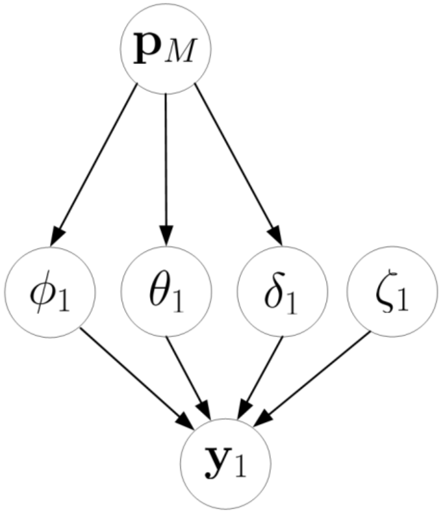

Anchor 1

Interplay between beam training and positioning

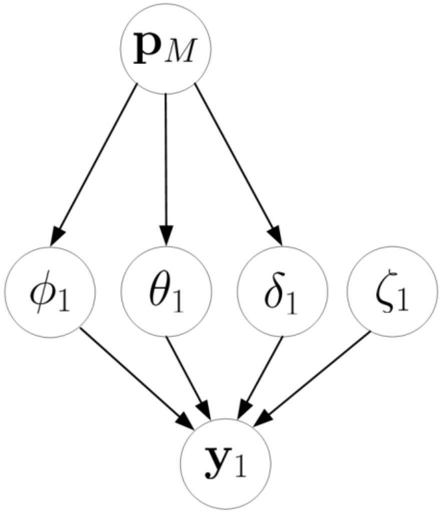

Anchor 1

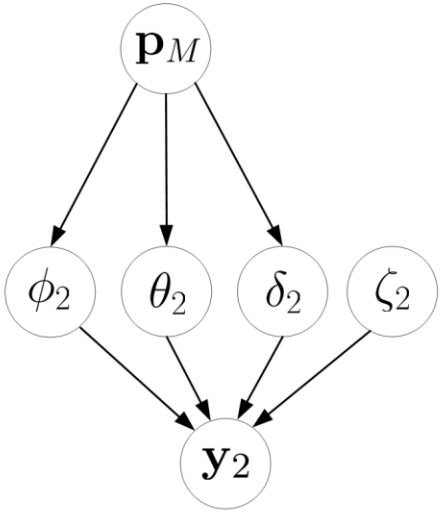

Anchor 2

Interplay between beam training and positioning

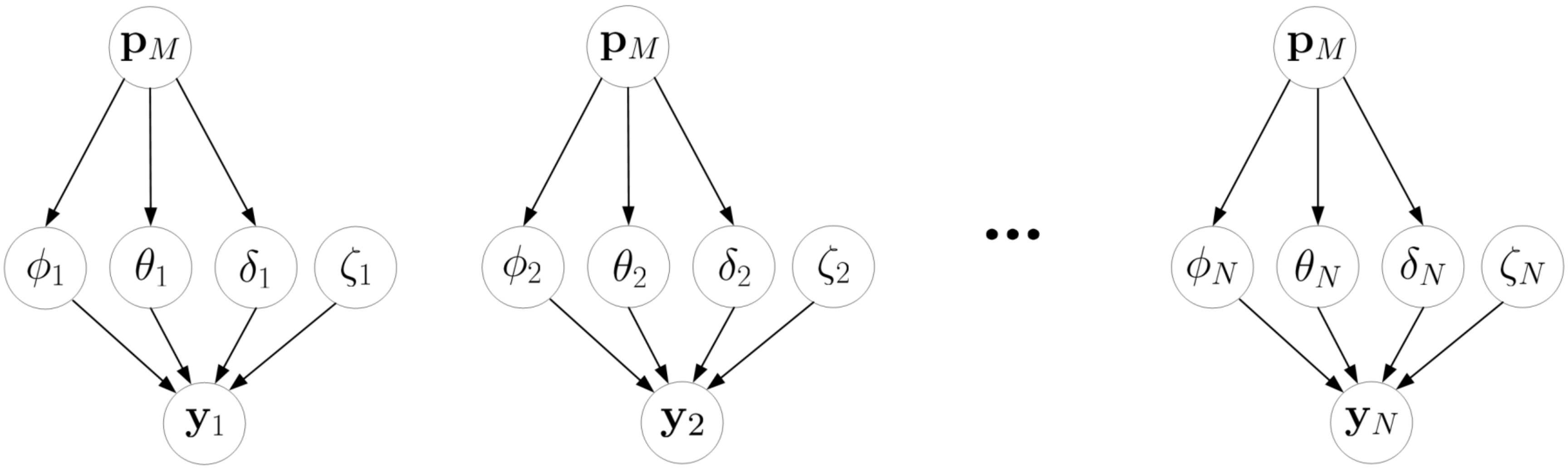

Anchor 1 **Anchor 2** **Anchor N**

Interplay between beam training and positioning

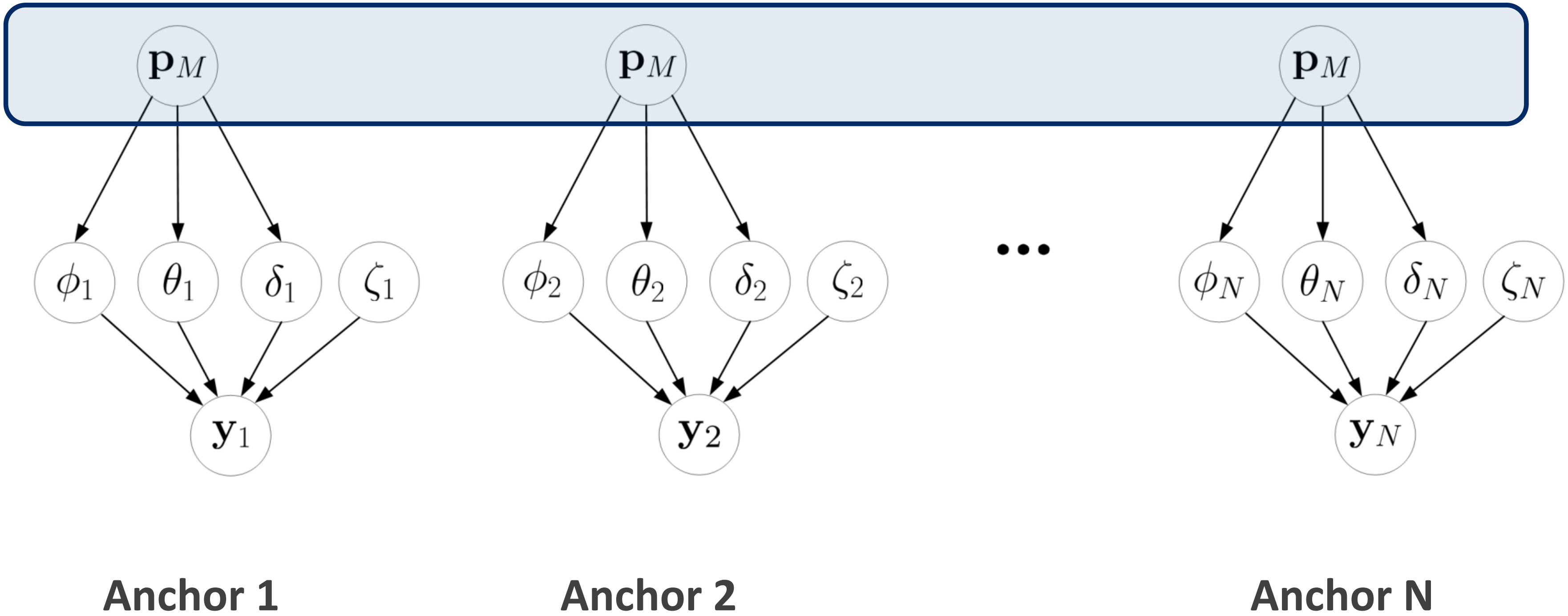

$\delta_n, \theta_n, \phi_n$ are conditioned on MT location $\mathbf{p}_M$.

Positioning

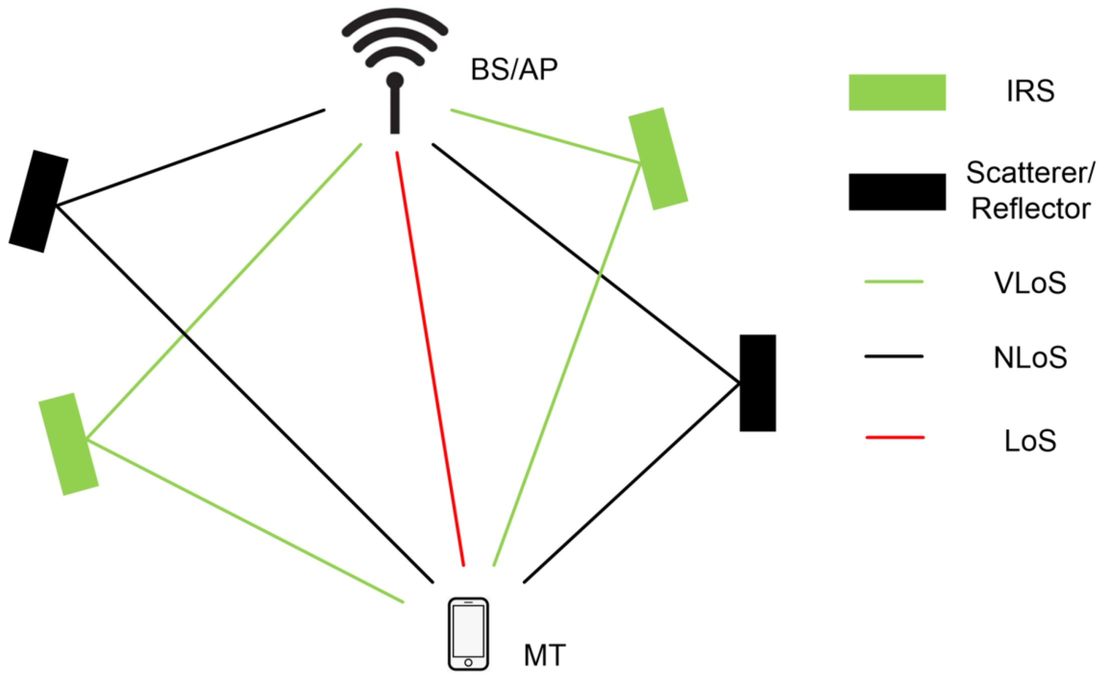

Positioning

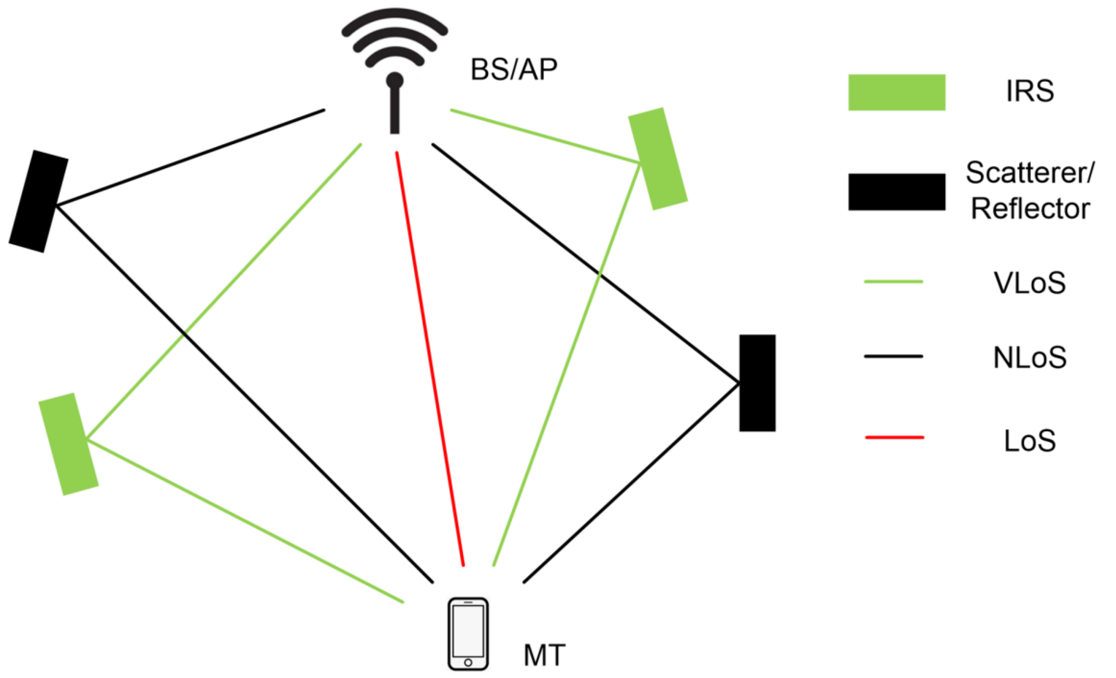

❖ Information of IRSs (i.e., reflector geometry, location) is available

Positioning

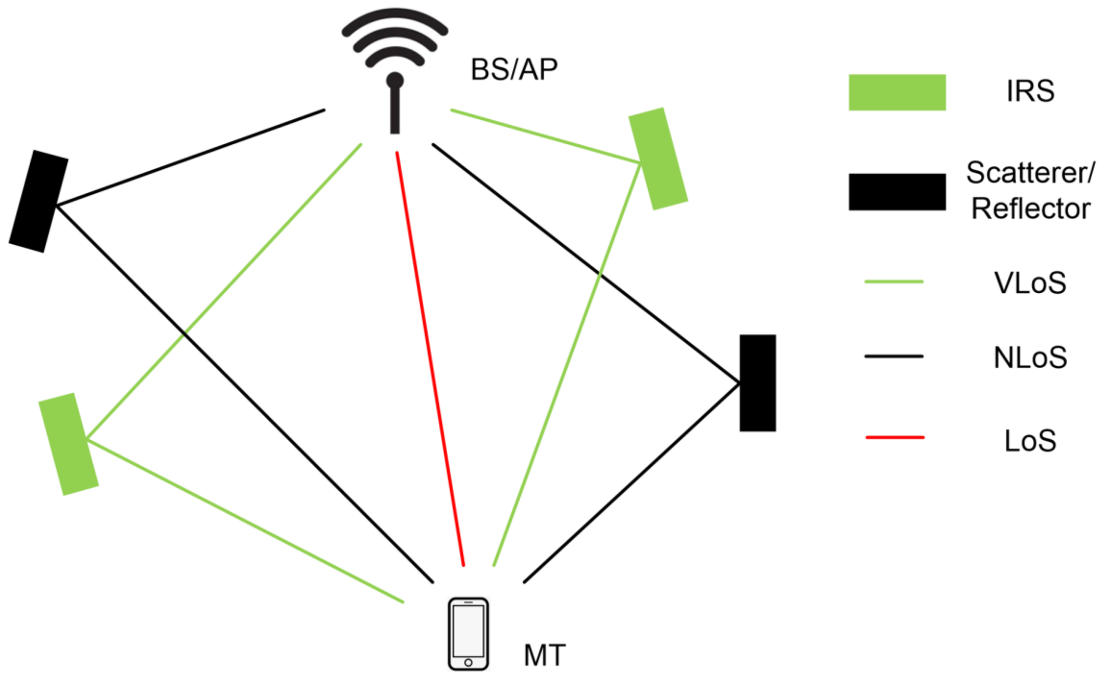

- Information of IRSs (i.e., reflector geometry, location) is available
- Information of BS/AP is available

Positioning

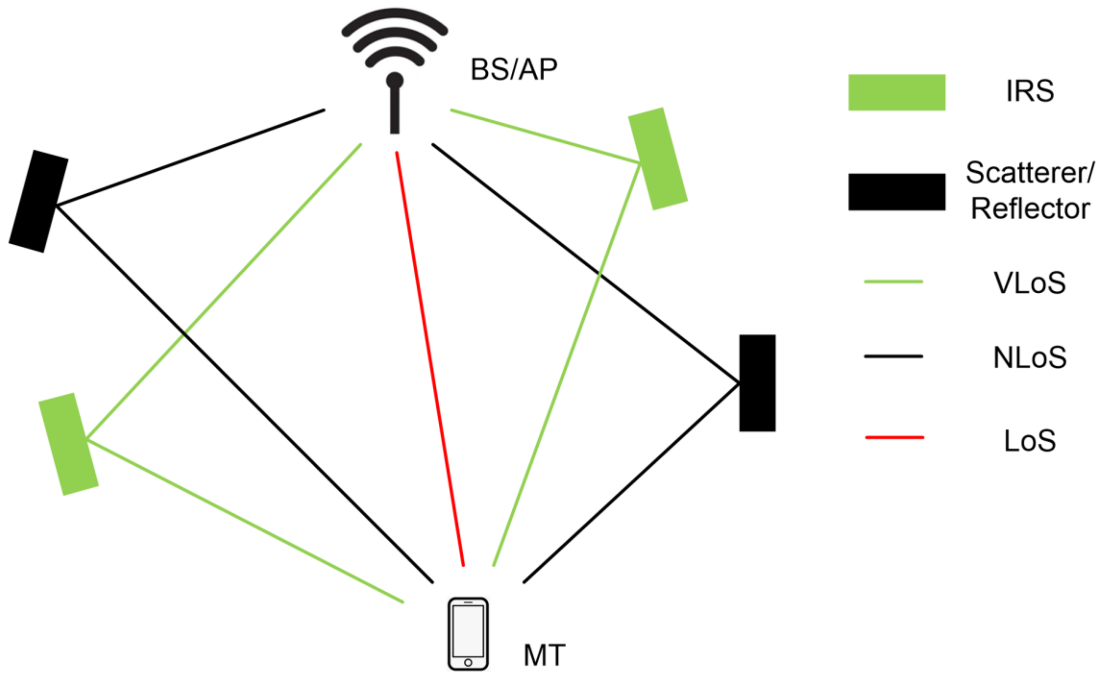

- ❖ Information of IRSs (i.e., reflector geometry, location) is available
- ❖ Information of BS/AP is available
- ❖ Treat BS/AP and IRSs as identical anchors
  - Three unblocked links (LoS/VLoS) are sufficient to estimate MT position

Positioning

- Sort the reliability of the anchors in ascending order according to

$$\varpi_n = \frac{\|\mathbf{y}_n - \hat{\delta}_n \mathbf{D}\mathbf{b}(\hat{\theta}_n, \hat{\phi}_n)\|_2^2}{\|\mathbf{y}_n\|_2^2}$$

- To estimate the 3-D position $\mathbf{p}_M$, least square criterion can be adopted

$$\min_{\mathbf{p}_M} \ \xi_\phi(\mathbf{p}_M) \triangleq \sum_{\eta \in \mathcal{N}} \left(\hat{\phi}_\eta - \frac{(\mathbf{p}_\eta - \mathbf{p}_M)^T \mathbf{e}_\eta}{\|\mathbf{p}_\eta - \mathbf{p}_M\|_2} \right)^2 \quad s.t. \quad \mathbf{p}_M \in \mathcal{S}$$

- Starting from the most reliable anchors, iteratively perform positioning algorithm until the algorithm fails to converge

Positioning – More Than a Fringe Benefit

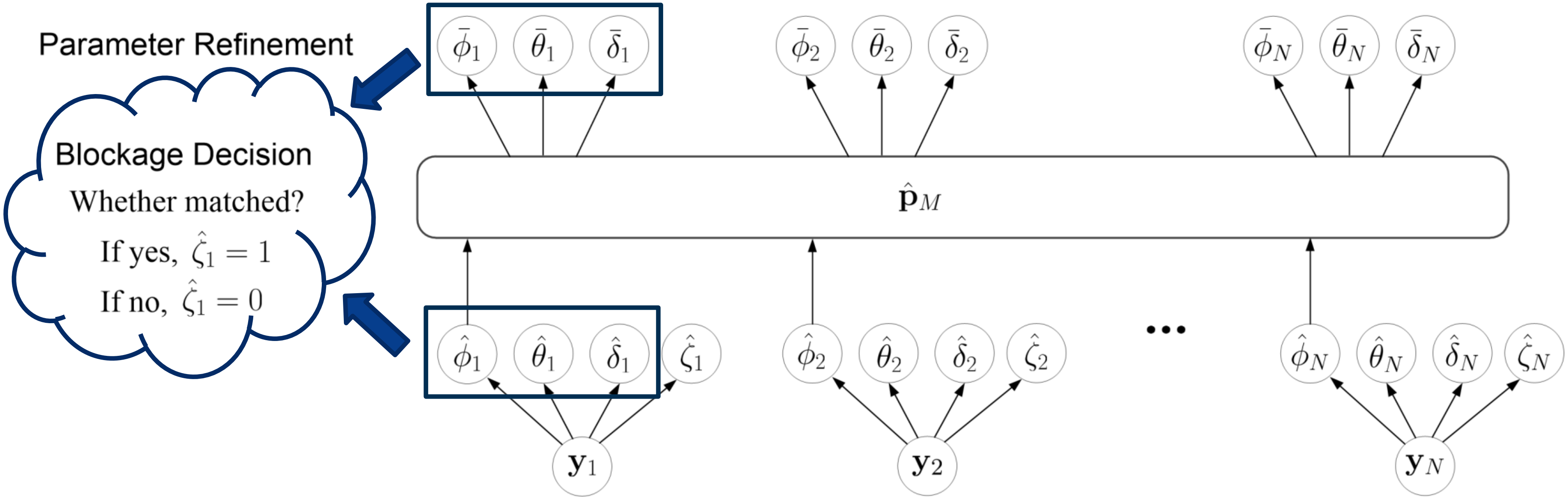

Positioning – More Than a Fringe Benefit

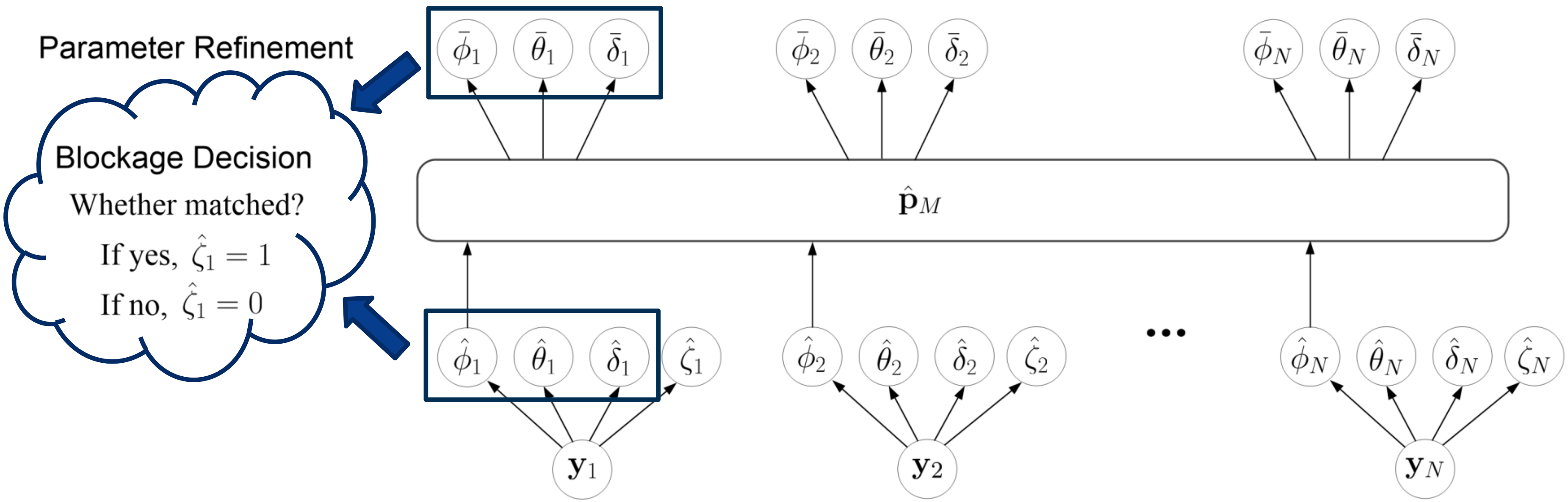

- Position aided parameter refinement: obtain $\bar{\delta}_n, \bar{\theta}_n, \bar{\phi}_n$ based on $\hat{\mathbf{p}}_M$
- Position aided blockage estimation: compare $\bar{\delta}_n$ (or $\bar{\theta}_n, \bar{\phi}_n$) with $\hat{\delta}_n$ (or $\hat{\theta}_n, \hat{\phi}_n$)

Outline

- ❑ Background and Motivation
- ❑ System Model
- ❑ Beam Training and Positioning
- ❑ Numerical Results
- ❑ Conclusion

Numerical Results

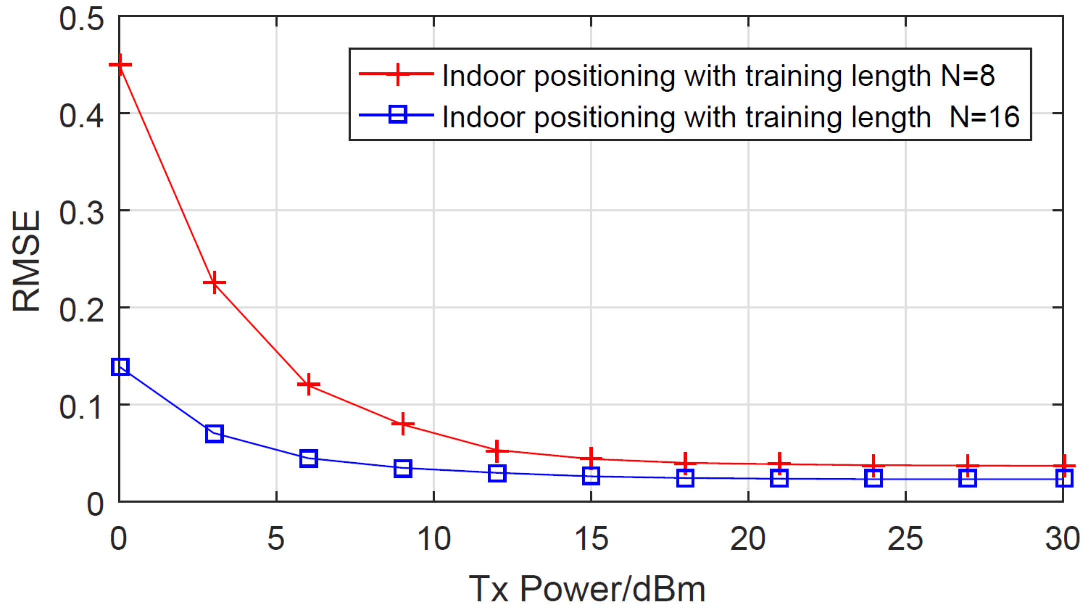

Fig. 6 Accuracy of Positioning

- When the training length is N=8, RMSE converges to 0.04 meter from 15 dBm.
- When the training length is N=16, RMSE converges to 0.02 meter from 15 dBm.

Numerical Results

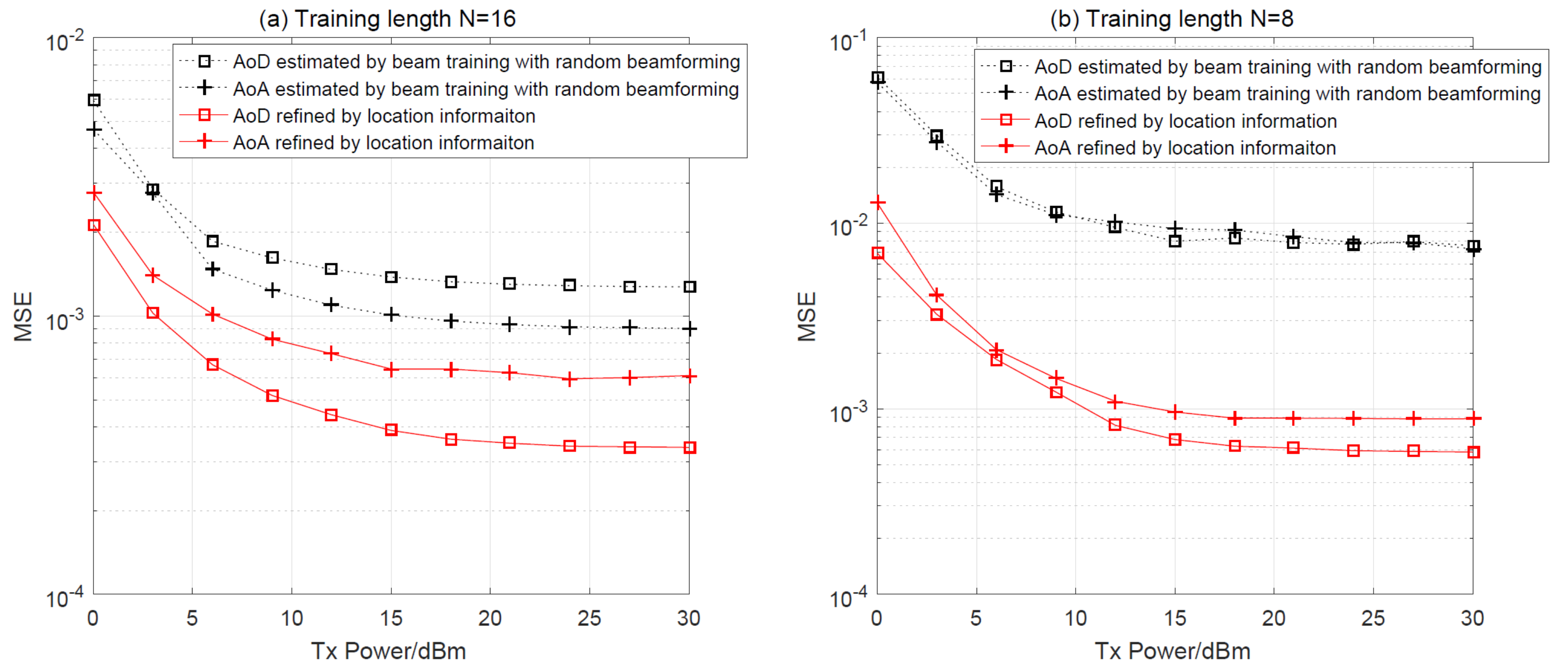

Fig. 7 MSE performance of AoA/AoD refined by location information

- Location aided parameter refinement significantly improves the accuracy of AoA/AoD estimation.

Numerical Results

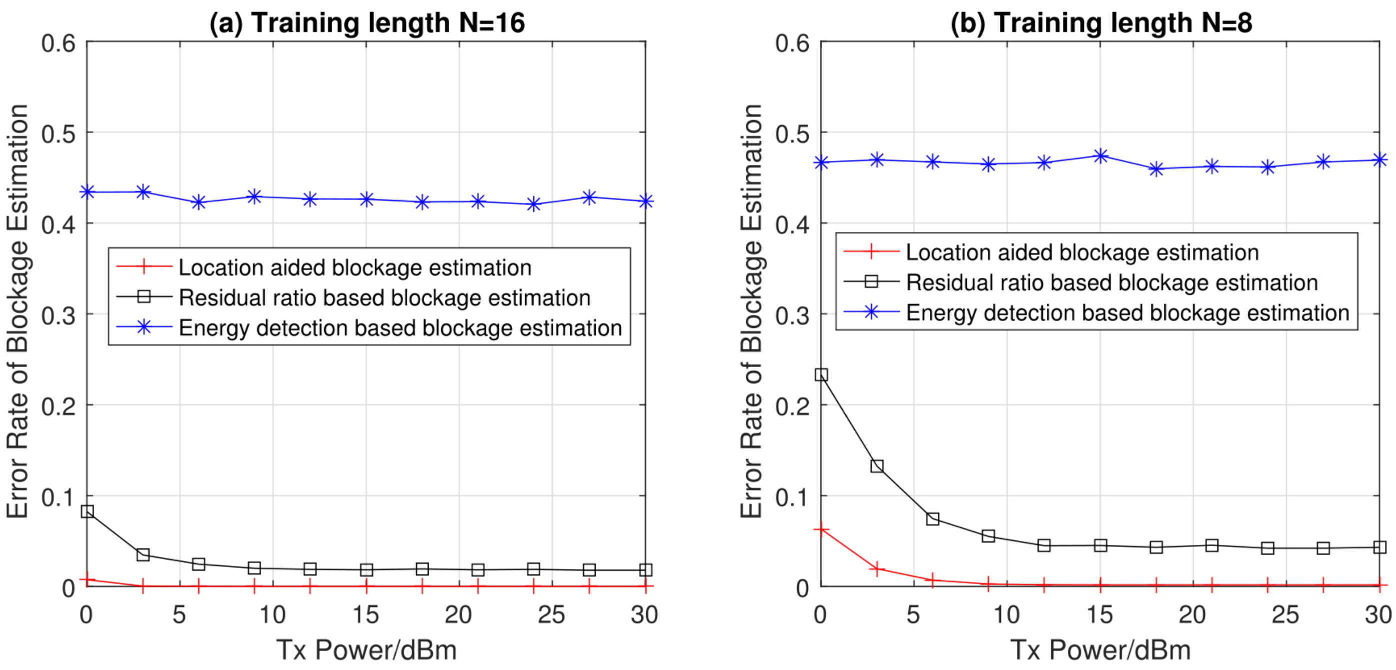

Fig. 8 Performance of blockage estimation

- Location aided blockage estimation outperforms traditional blockage estimation methods

Outline

- Background and Motivation
- System Model
- Beam Training and Positioning
- Numerical Results
- Conclusion

Conclusion

- With IRSs, we can artificially configure the wireless channel

- Using compressed sensing techniques, we accurately estimate the parameters of the LoS/VLoS paths, which facilitates localization of MTs

- With the aid of location information, we cross verify and enhance the parameters of the LoS/VLoS paths.